JOURNAL OF AIRCRAFT
Vol. 37, No. 1, January–February 2000

Predicting Glaze or Rime Ice Growth on Airfoils

Marcia K. Politovich*
National Center for Atmospheric Research, Boulder, Colorado 80307

A droplet trajectory analysis model is combined with calculations of heat transfer to provide predictions of glaze or rime ice during flight. Such a prediction is not currently available and could prove useful for flight planning. The droplet trajectory model is used to determine the collection efficiency of various sized cloud droplets on representative airfoils. This information is included in ice accretion and growth calculations to determine whether wet (usually glaze or mixed icing) or dry (rime icing) growth is expected for combinations of outside air temperature, liquid water content, and impinging droplet size. The calculations produced critical liquid water contents for the rime to glaze transition that varied from 0.15 ± 0.051 g/m^3 for a Cessna T-37B to 0.38 ± 0.154 g/m^3 for a Beechcraft Queen Air at their typical airspeeds and for atmospheric conditions 700 hPa, −10°C, and 15-μm impinging droplets. For larger droplets, lower atmospheric pressure, and higher airspeeds these critical values decreased, making glaze more likely. Suggestions for adaptation of the calculations as guidelines for forecasting icing type are presented.

Nomenclature

c_p = specific heat of dry air at constant pressure
c_w = specific heat of water at 0°C
D = collector diameter
e = saturation vapor pressure at T
e_0 = saturation vapor pressure at 0°C
k = R_d / R_v
k_a = molecular thermal conductivity of air
L_e = latent heat of evaporation
L_f = latent heat of fusion
n = 8.1×10^7 K^3
P = air pressure
q_c = loss of sensible heat to air
q_e = evaporative heat loss
q_f = latent heat of fusion
q_k = kinetic energy of droplets
q_l = heat loss to the substrate due to conduction
q_r = heat lost to warming the runoff water
q_s = heat loss due to radiation
q_v = frictional heating of air
q_w = heat loss in warming freezing accreted water to 0°C
r = recovery factor for viscous heating (= 0.9)
T = outside air temperature, °C
V = airspeed
$\beta_{\max}$ = maximum collection efficiency of collector (at or near stagnation point)
β_{tot} = total collection efficiency of collector
μ_a = molecular viscosity of air
ρ = air density
σ = Boltzmann constant

Introduction

IN-FLIGHT icing is the accretion of supercooled liquid water on an aircraft during flight. The shape and location of the accreted ice depends on both meteorological and aircraft-specific factors, including outside air temperature, liquid water content, droplet size, airspeed, the shape of the accreting surface (including flap configuration, etc.), and ice protection devices such as heated surfaces or pneumatic boots.

The accreted ice can grow through either a wet or dry growth process. In a dry growth process, impacting droplets freeze nearly immediately on impact. The droplets are able to lose the latent heat of fusion rapidly and so they freeze in place and maintain their nearly spherical shape. The accretion is thus filled with air spaces between the frozen drops, and the appearance of the low-density (typically < 0.5 g/cm^3) (Ref. 1) brittle ice is white and opaque. Rime ice accretions tend to form forward into the airstream.

During wet growth the droplets are unable to release latent heat of fusion quickly. The droplets deform and run aft along the airframe or flow between frozen drops in a previously collected wet growth accretion. The accretion is denser than dry-growth ice and the appearance is more glossy and translucent, even clear in thin accretions.

Dry growth is generally associated with rime ice and wet growth with clear or glaze ice (in this paper the term glaze will be used). Mixed icing represents a transition between wet and dry growth, or glaze and rime ice. In a general sense, the conditions that favor dry growth are those favoring the rapid release of latent heat from the impacting droplets: colder temperatures and lower liquid water contents. Conversely, higher amounts of liquid water and warmer temperatures favor wet growth. Airspeed, the collector shape and size, and the size of the impacting droplets enter into the process as well. However, with some assumptions about typical droplet sizes expected in clouds and about typical aircraft parameters, we can use the relation of wet or dry growth to temperature and liquid water content to enable predictions of icing type to be made.

The approach used in this study is to combine output from an airfoil trajectory model with heat-balance calculations to determine the likelihood of glaze or rime ice for a variety of aircraft. Environmental conditions typical of those expected in icing conditions are applied.

Temperature and liquid water fields are available from numerical weather forecast models run operationally at the National Center for Environmental Prediction. Liquid water content has not yet been verified as reliably accurate, and droplet size is not currently predicted. However, as pointed out in a climatological study of icing conditions,[2] 75% of mean droplet diameters recorded by research aircraft flying in various seasons and geographical areas in North America were in the range 10–20 μm, and so a 15-μm estimate for mean droplet size may be adequate for forecast applications. Some implications of uncertainty in droplet sizes in clouds will be addressed in this paper.

Glaze vs rime icing calculations could be included in icing forecasts in several ways depending on the needs of the end user. The format could be a plan view or cross section along the planned route of flight such as presented by the Aviation Weather Center's Aviation Digital Data Service.[3] Other formats, such as will be presented later in the paper, could be used to look up the expected icing type

Received 2 March 1999; revision received 8 July 1999; accepted for publication 27 July 1999.

*Project Scientist, P.O. Box 3000, Research Applications Program; marcia@ucar.edu.

Table 1 Airplanes and parameters used in this study

Airplane	Airfoil (from Jeck[4])	Airfoil used in trajectory program	Chord, m	Equivalent airfoil diameter, m	V, m/s	Angle of attack, deg
3-in. cylinder	3-in.-diam cylinder	Circle	0.0762	0.0762	89.4	0.0
QA	NACA-23012	NACA-23015	1.07	0.161	77.2	3.0
Beechcraft 1900D	NACA-23012	NACA-23015	0.91	0.137	103.9	2.9
Ct37	NACA-2410	NACA-2412	1.7	0.204	128.4	0.0
C640	NACA 23015	NACA 23015	1.4	0.210	128.4	1.3
P3	NACA-0012 (mod)	NACA-0012	2.31	0.277	128.4	2.1

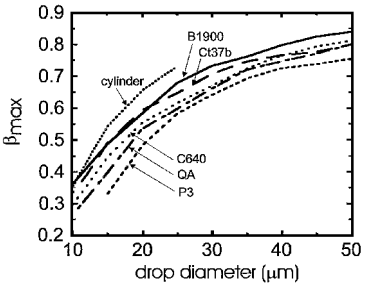

Fig. 1 Maximum collection efficiency β_{max} plotted against droplet diameter; characteristics for the cylinder and aircraft are listed in Table 1.

from already-existing numerical weather model output. The most rigorous application would be to use aircraft-dependentparameters specifically for the aircraft of interest. This could be used, for example, in an airline dispatch office or military forecast office, where staff are concerned with a limited set of airplane types. For more general use, choices representing different aircraft classes such as small general aviation, larger general aviation, regional propeller aircraft, small and large jets, etc., could be made, with different products tailored for these users.

Maximum Impingement Efficiency Calculations

For this study, the accretion of supercooled liquid drops on an airfoil during flight are considered. Jeck[4] provides a summary of information pertinent to this problem for typical airfoil and airspeed combinations. A subset of these conditions used in this study is listed in Table 1. A variety of aircraft is represented here. The Lockheed P-3 Orion (P3) is a large, four-engine propeller aircraft flown in coastal surveillance and by the National Oceanic and Atmospheric Administration for hurricane and other weather research. The Beechcraft 1900 (B1900) is a 19-passenger, twin-turboprop commuter aircraft. The slightly smaller Queen Air (QA) has two piston engines. The Convair 640 (C640) is a 40–50 passenger twin turboprop or piston engine aircraft, and the Cessna T-37 (Ct37) is a twin-engine military jet trainer. The 3-in. (0.0762-m) cylinder is used as a comparison.

Jeck[4] calculated β_{tot}, the maximum collection efficiency on the entire airfoil surface, for 15-μm droplets. This study is concerned with conditions at or near the stagnation point of the airfoil, where β_{tot}, referred to here as β_{max}, is the appropriate value. A droplet trajectory program[5] was used to obtain β_{max}. The program calculates the impingement of cloud-sized (10–50 μm diameter) droplets on single-element airfoils and uses a Lagrangian method to calculate a series of individual droplet trajectories from five chord lengths upstream of the airfoil to impact with the surface. Only monodisperse droplet size distributions are modeled in the program. However, it has been shown[6] that the collection efficiency for realistic cloud droplet size distributions is well represented by that of the median volume diameter of the distribution.

Limits on k_0, the modified inertia parameter, limit the droplet sizes, temperature, and pressure ranges used for input to the program for some collector shapes. A limited number of airfoils are available for the calculations and these were matched as closely as possible to those used by Jeck[4] for the study aircraft.

Typical airspeeds and angles of attack for the six airfoils listed in Table 1 were taken from Jeck[4] and entered into the trajectory program. Figure 1 shows the effect of droplet diameter on β_{max} for the six airfoils. These calculations were run for 700-hPa pressure and a temperature of −10°C. Although the cylinder has the slowest airspeed, it also has the smallest diameter, which results in the highest β_{max}. The P3, with its thick wing and relatively high airspeed has the lowest β_{max}. Other aircraft lie between these values.

Table 2 β_{max} and W_c at 700 hPa, 10°C; all calculations are for 15 μm except where noted

Airplane	β_{max}	W_c, g/m^3	σ_{W_c} / W_c
3-in. cylinder	0.54 ± 0.156	0.36 ± 0.116	0.29
QA	0.43 ± 0.115	0.38 ± 0.154	0.38
Beechcraft 1900D @ 10 μm	0.36 ± 0.124	0.34 ± 0.172	0.51
Beechcraft 1900D @ 15 μm	0.51 ± 0.107	0.24 ± 0.071	0.24
Beechcraft 1900D @ 25 μm	0.68 ± 0.0808	0.18 ± 0.0407	0.22
Beechcraft 1900D @50 μm	0.84 ± 0.0360	0.14 ± 0.0305	0.21
Ct37	0.49 ± 0.106	0.15 ± 0.051	0.25
C640	0.45 ± 0.104	0.16 ± 0.058	0.29
P3	0.33 ± 0.132	0.15 ± 0.067	0.46

Because the trajectory analysis program is complex, uncertainties in β_{max} were estimated using the following method. The program was run for the airfoil shapes at ranges of velocity V, temperature T, and pressure P that would normally be encountered during flight. All three parameters had approximately linear relations to β_{max} in the ranges of V(±10 m/s around the value listed in Table 1), T (−25–0°C) and P (400–900 hPa) used (see Fig. 2) when all other parameters were held constant. Environmental conditions were P = 700 hPa, T = −10°C and droplet diameter = 15 μm unless otherwise noted. The slopes of the lines were similar for the different airfoils and for three droplet sizes (15, 25, and 50 μm) of the B1900. The slopes can be used in a standard error analysis treatment that uses the partial differentials with respect to the variables and their expected errors in the form

$$\sigma_\beta = \sum \left(\frac{\partial \beta}{\partial i}\right)\left(\frac{\partial \beta}{\partial j}\right)\sigma_i \sigma_j \qquad (1)$$

where i and j are the variables V, T, P, and droplet diameter; $\partial b/\partial i$, j are the partial differentials of β_{max} for each variable; and $\sigma_{i,j}$ are the expected errors in the variables. For this analysis errors were assumed to be uncorrelated. Errors for V, T, and P were assumed to be 10 m/s, 2°C, and 10 hPa, respectively, and represent ranges of values expected during level flight and, in the case of the meteorological variables, possible uncertainties in their prediction. Other aircraft parameters such as airfoil size, shape, and angle of attack were assumed constant. In level flight there will be some variation in angle of attack, but this is assumed to be small.

The error resulting from uncertainty in droplet diameter was estimated by fitting a second-order polynomial to the β_{max} vs. diameter curves shown in Fig. 1 (all had correlation coefficients of at least 0.99) and assuming an uncertainty or error in diameter of 5μm.

Propagating these errors provides the values shown in Table 2. The largest contributor is the droplet diameter term because β_{max} changes considerably with droplet diameter but more slowly with the other variables. Errors for the cylinder and P3 are largest because their diameter vs. β_{max} curves (Fig. 1) are steeper than those of the other aircraft. Errors were also estimated for droplet diameters of 10, 25, and 50 μm for the B1900, which shows that the errors in β_{max} decrease with increasing droplet diameter.

Wet and Dry Ice Growth Calculations

As already mentioned, icing type (rime, glaze, or mixed) depends on a number of meteorological and aircraft-specific factors.

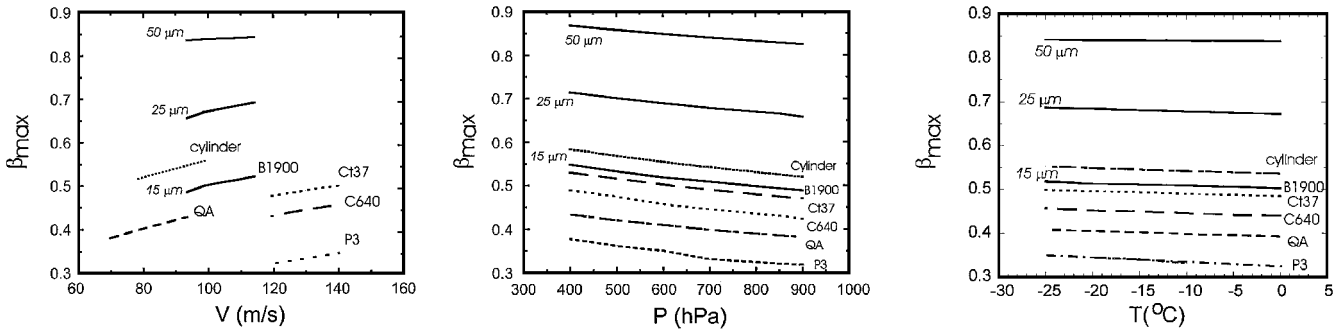

a) Velocity V b) Pressure P c) Temperature T

Fig. 2 Effects of input parameters on β_{max}.

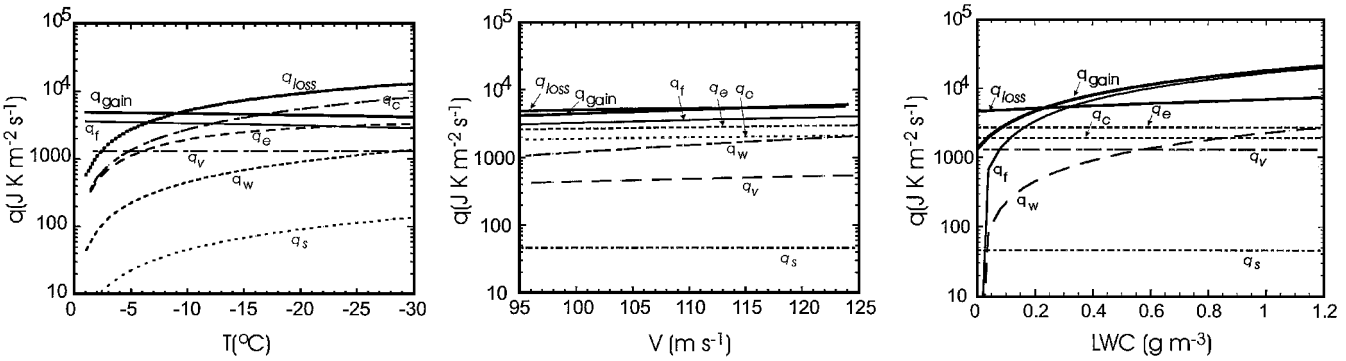

a) Outside air temperature T b) Airspeed V c) LWC

Fig. 3 Heat loss and gain terms from Eq. (2) plotted against.

Makkonen[7] describes both wet and dry growth regimes in calculating growth rates of ice deposited on wires. He describes a transition from wet to dry growth based on a critical liquid water content W_c, for given, fixed values of other parameters such as airspeed and collection efficiency. The problem is one of heat transfer, whether the latent heat of fusion is dissipated quickly enough to freeze droplets immediately after impact, rather than forming a liquid surface prior to freezing.

The balance is between heat gained and lost on the ice surface, or

$$q_{\text{gain}} = q_{\text{loss}}$$

or

$$q_f + q_v + q_k = q_c + q_e + q_w + q_r + q_s + q_l \qquad (2)$$

The terms are defined as by Makkonen.[7] Figure 3 shows their relative importance and their dependence on outside air temperature T, pressure P, and airspeed V. For these calculations, T, V, and liquid water content (LWC) were held at −10°C, 103.9 m/s, and 0.2 g/m^3 (except when these parameters were varied) to simulate winter conditions encountered by a B1900.

The total heat gain term q_{gain} increases with T, V, and LWC. The dependence on T is realized through increases in the latent heat of fusion and molecular conductivity with temperature. The latent heat of fusion was adjusted for temperature by using a best-fit, second-order polynomial to the data given by Iribarne and Godson[8]; molecular conductivity was calculated using the formula of Beard and Pruppacher.[9] The q_f term that represents latent heat of fusion is strongly dependent on LWC, whereas q_v, the frictional heating of air, is not. The summed heat loss term q_{loss} decreases with T. Heat loss is generally independent of LWC except for q_w, the heat lost in warming the freezing water mass to 0°C. The loss of sensible heat to surrounding air q_c increases with decreasing T, but is only weakly dependent on V and independent of LWC. The evaporative heat loss q_e behaves similarly to q_c, but is not as strongly dependent on T. The term q_w is generally smaller than q_c and q_e except at high LWC. The heat loss due to radiation q_s is generally small compared to the other q_{loss} terms.

Three terms are neglected in this study: q_k, the kinetic energy of the droplets themselves; q_r, the heat lost to runback water; and q_l, the conductive heat loss through the aircraft surface. The droplets are assumed to be nearly stationary with fall speeds on the order of centimeters per second, and horizontal speeds in clouds on the order of meters per second. At the stagnation point of the airfoil, it is assumed there is no runback water (all water either freezes or remains liquid at that point on the airfoil. It is also assumed that droplets do not bounce off the surface. Heat conduction through the airfoil surface is neglected; the case of a heated, anti-iced wing will not be considered here, nor will the case of cold soaking.

The differing dependences of q_{gain} and q_{loss} on T, V, and LWC as well as other parameters results in $q_{\text{gain}} > q_{\text{loss}}$ (wet growth) in some conditions and $q_{\text{gain}} < q_{\text{loss}}$ (dry growth) in others, as illustrated in Fig. 3. The difference between wet and dry growth can be more readily summarized by one variable, W_c, the critical liquid water content. W_c is obtained by equating the heat gain and loss terms, $q_{\text{gain}} = q_{\text{loss}}$, along with the assumption that at or near the stagnation point the Nusselt number is approximately the square root of the Reynolds number.[10] The full derivation of W_c is described by Makkonen[7] and will not be repeated here. The final expression for W_c becomes

$$W_c = k_a/\beta_{\max}(\rho/V/D/\mu)^{\frac{1}{2}}\left[-T + kL_e(e_0 - e)/c_p/P - rV^2/2/c_p\right]/(L_f + c_w T) - \sigma n T/[\beta_{\max} V(L_f + c_w T)] \qquad (3)$$

Two groups of variables are embedded in Eq. (3). The first group is related to the environment through pressure and temperature. The second group is related to the specific aircraft under consideration through the maximum collection efficiency $\beta_{\max}$ that is also related to the droplet size, the airspeed, and the effective diameter of the collector. It is certainly possible that two aircraft, with different airfoils and airspeeds, can fly through the same environmental conditions and encounter different icing types.

Figure 4 shows the critical LWC W_c vs temperature for the aircraft types at their typical conditions in Table 1 and 700 hPa. The cylinder and QA have the highest W_c for a given temperature. The Ct37, P3, and C640 have the lowest W_c at all droplet sizes. The B1900 is

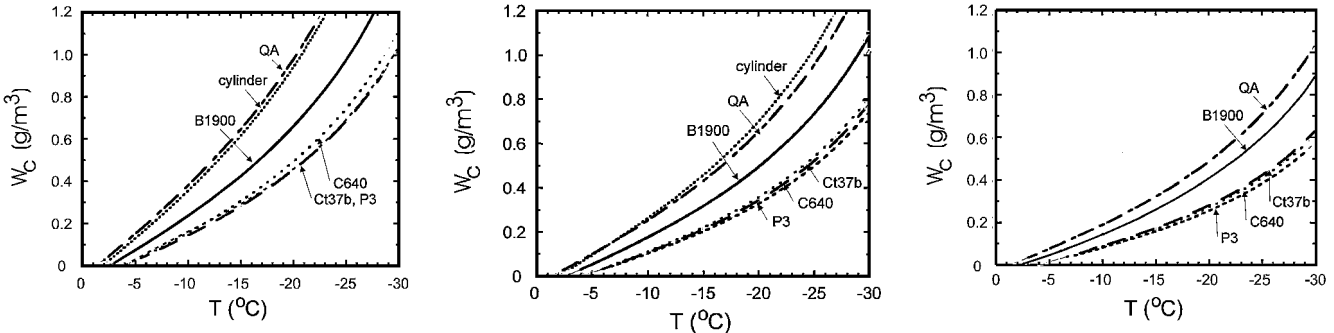

a) 15-μm droplet diameter b) 25-μm droplet diameter c) 50-μm droplet diameter

Fig. 4 Critical LWC W_c, plotted against temperature for the test airfoil types listed in Table 1.

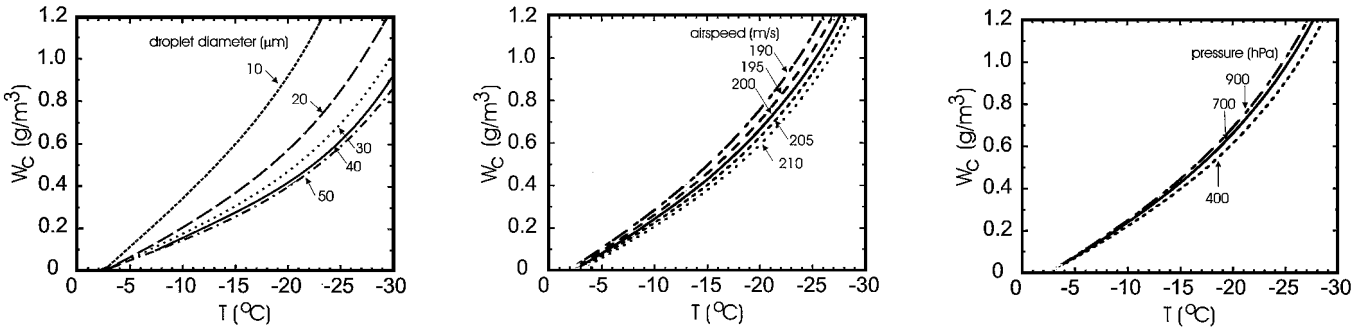

a) Droplet diameters from 10 to 50 mm b) Airspeed from 190 to 210 m/s c) Pressure from 400 to 900 hPa

Fig. 5 Effects of parameters on W_c for the B1900.

between the two groups. Larger droplets result in lower W_c for any given temperature, that is, icing is more likely to be glaze given the same LWC and T if larger droplets are encountered.

The effects of parameters contributing to W_c are shown for the B1900 in Figs. 5a–5c. W_c decreases with increasing droplet diameter as was suggested in Fig. 4. W_c also decreases with increasing airspeed; as more heat due to adiabatic compression is generated at the stagnation point delaying the freezing process, glaze icing is more likely there. Additionally, $\beta_{\max}$ increases, allowing for more water mass to be collected. Given the same outside air temperature, W_c increases with increasing pressure, although the differences are slight. At lower pressure there is less bow-wave effect allowing more droplets to impinge on the airfoil, creating more mass freezing and more latent heat released.

Errors were propagated to estimate uncertainties in W_c using standard methods. Atmospheric variables are ρ, μ_a, T, L_e, e_0, e, P, and L_f. The quantities μ_a, L_e, e_0, e, and L_f are slowly varying functions of T and their variations are small and will be neglected, leaving T and P (ρ is directly related to T and P and W_c can be rewritten as such). Partial derivatives of W_c with respect to T, P, V, and E can be calculated from Eq. (3) analytically. The same error estimates for T, P, and V as used in the error estimates for $\beta_{\max}$ were assumed, and the error in $\beta_{\max}$ described in an earlier section was propagated through. Figure 6 shows $W_c + \sigma_{W_c}$ for the QA and P3 at 700 hPa, −10°C, and 15-μm droplet diameter. These had the highest and lowest ranges of all of the test aircraft listed in Table 2.

Another presentation of the W_c information is illustrated in Fig. 7, which shows droplet size (either as a single diameter, or interpreted as the median volume diameter) plotted against temperature. W_c are shown as isolines. For example, for an environment with 18-μm droplets at −6°C, glaze icing would be expected if the LWC exceeded 0.1 g/m^3, whereas at a lower temperature of −18°C, LWC must exceed 0.5 g/m^3 for glaze to form. As with Fig. 4, no account is made here for uncertainties in W_c arising from uncertainty in the other parameters. A way in which these uncertainties might be utilized is shown in Fig. 8. This plots W_c vs T as in Fig. 4, but uses the maximum and minimum $W_c + \sigma_{W_c}$ lines from Fig. 8 (maximum was $W_c + \sigma_{W_c}$ for the QA, minimum was $W_c - \sigma_{W_c}$ for the P3) to bound

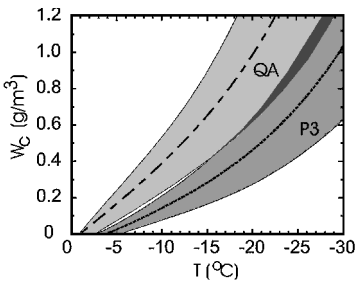

Fig. 6 $W_c \pm \sigma_{W_c}$ for the QA and P3 at 700 mb, −10°C, and 15 μm; shaded areas represent the $\pm\sigma_{W_c}$ boundaries; darker shading is where the values overlap.

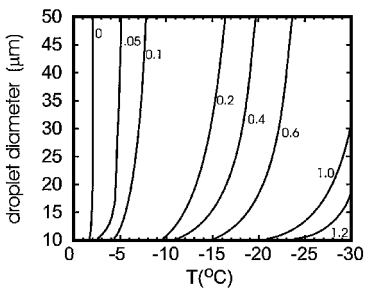

Fig. 7 W_c as a function of droplet diameter and temperature.

confidence limits for the determination of glaze or rime ice. Points lying above the maximum $W_c + \sigma_{W_c}$ line are designated glaze, below the minimum $W_c - \sigma_{W_c}$ line are rime, and those in between are mixed icing. Also shown on Fig. 8 are the trace, light, moderate, and severe icing categories as defined by Lewis,[11] so that if air temperature and liquid water content are known or estimated, the type and severity of expected icing could be predicted. Note that this is for an assumed droplet diameter of 15 μm (Lewis's[11] assumption was 14 μm); the envelopes will move up (more rime expected) with smaller drops and will move down (more glaze expected) with larger drops.

Figure 9 shows W_c for the B1900 for 10–20 μm droplets plotted with data points from the University of Wyoming King Air research aircraft. These data points were obtained during flights in the Great

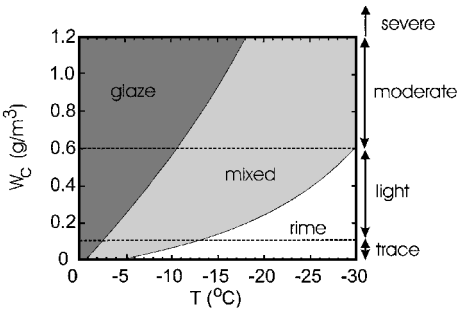

Fig. 8 Critical LWC W_c plotted against temperature T; expected glaze, mixed, and rime icing conditions are noted as in the text; icing severity is shown at the right of the plot.

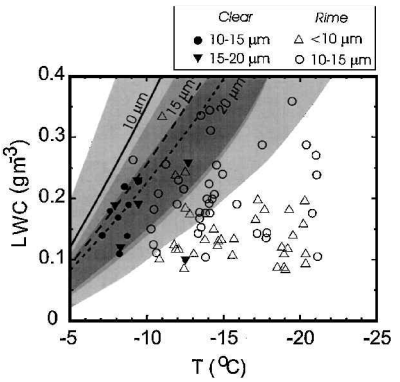

Fig. 9 W_c for the B1900 for 10–20 μm droplets plotted with data points from University of Wyoming King Air research flights in the Great Lakes and Great Plains in winter 1980–1981; shading denotes $W_c \pm \sigma_{W_c}$ for the droplet diameters indicated.

Lakes and Great Plains area in winter 1980–1981 (Ref. 12). Droplets were typically small (median volume diameters in this sample set were all <20 μm) and LWC were low (<0.4 g/m^3). The flight crew noted the ice type (as glaze or rime, no observations of mixed were recorded) for each of a series of icing encounters. Most observations were of the leading edge of the wings, which are clearly visible from the cockpit of the airplane. The average LWC and T of each encounter, which usually spanned several minutes of flight, were recorded. The data points were stratified by the median volume diameters of the droplet size distributions. Most of the observations are in reasonable agreement with the prediction from this study, assuming that wet growth leads to glaze icing and dry growth to rime. The error boundaries for 10-, 15-, and 20-μm drops are shown as shaded areas on the diagram.

Conclusions

Glaze and rime ice accretion for six airfoils in a range of environmental conditions were explored. Results from an airfoil trajectory model were combined with calculations of heat transfer from the accreted supercooled liquid to the atmosphere to arrive at a prediction of either glaze or rime ice. The results quantify the qualitative relations expected for glaze and rime growth; wet growth, leading to glaze, is favored by warmer temperatures and higher LWCs. Larger droplets make more water available to accrete on the airframe; thus, a transition between dry and wet growth occurs at lower LWC if large droplets are present. Critical LWCs for the rime to glaze transition varied from 0.15 ± 0.051 g/m^3 for a Ct37 to 0.38 ± 0.154 g/m^3 for a QA at their typical airspeeds and angles of attack and for atmospheric conditions 700 hPa, -10°C, and 15-μm impinging droplets.

The method may be readily adapted to forecasting using numerical weather model output that includes temperature and LWC.

Acknowledgments

This study was supported primarily by the NASA Advanced General Aviation Transport Experiment Ice Protection Package. Additional support was obtained from the National Science Foundation through an interagency agreement in response to requirements and funding by the Federal Aviation Administration's Aviation Weather Development Program. Many thanks also go to the flight crew of the Wyoming King Air for data collection in potentially hazardous conditions.

References

[1]Macklin, W. C., "The Density and Structure of Ice Formed by Accretion," *Quarterly Journal of the Royal Meteorological Society*, Vol. 88, No. 1, 1962, pp. 30–50.

[2]Jeck, R., "A New Database of Supercooled Cloud Variables for Altitudes up to 10,000 Feet AGL and the Implications for Low Altitude Aircraft Icing," U.S. Dept. of Transportation Rept. DOT/FAA/CT-83/21, Washington, DC, 1983.

[3]Sherretz, L. A., Thompson, G., and Mahoney, T., "Overview of the Aviation Digital Data Service," *Preprints of the Eighth Conference on Aviation, Range and Aerospace Meteorology*, American Meteorology Society, Boston, 1999, pp. 134–137.

[4]Jeck, R., "A Workable, Aircraft-Specific Icing Severity Scheme," AIAA Paper 98-0094, Jan. 1998.

[5]Bragg, M. B., "The Effect of Geometry on Airfoil Icing Characteristics," *Journal of Aircraft*, Vol. 21, No. 7, 1984, pp. 505–511.

[6]Finstad, K. J., Lozowski, E. P., and Makkonnen, L., "On the Median Volume Diameter Approximation for Droplet Collision Efficiency," *Journal of the Atmospheric Sciences*, Vol. 45, No. 1, 1988, pp. 4008–4012.

[7]Makkonen, L., "Estimating Intensity of Atmospheric Ice Accretion on Stationary Structures," *Journal of Applied Meteorology*, Vol. 20, No. 5, 1981, pp. 595–599.

[8]Iribarne, J. V., and Godson, W. L., *Atmospheric Thermodynamics*, D. Reidel, Boston, 1981, p. 246.

[9]Beard, K. V., and Pruppacher, H. R., "A Wind Tunnel Investigation of Collection Kernels for Small Water Drops in Air," *Quarterly Journal of the Royal Meteorological Society*, Vol. 97, No. 4, 1971, pp. 242–248.

[10]Schlichting, H., *Boundary Layer Theory*, McGraw–Hill, New York, 1979, p. 305.

[11]Lewis, W., "A Flight Investigation of the Meteorological Conditions Conducive to the Formation of Ice on Airplanes," NASA TN-1393, 1947.

[12]Sand, W. R., Cooper, W. A., Politovich, M. K., and Veal, D. L., "Icing Conditions Encountered by a Research Aircraft," *Journal of Climate and Applied Meteorology*, Vol. 23, No. 10, 1984, pp. 1427–1440.